

# Resonantly Excited Normal Modes and Shear Melting of a Nonequilibrium Pattern

Daniel I. Goldman,\* M. D. Shattuck, Sung Joon Moon, J. B. Swift, and Harry L. Swinney  
 Center for Nonlinear Dynamics, The University of Texas at Austin, Austin, TX 78712  
 (Dated: October 27, 2019)

We find that the square patterns formed in a vertically oscillating granular layer exhibit dynamics like those of a two-dimensional (2D) square lattice coupled by Hookian springs. Different transverse normal modes of the granular lattice are resonantly excited for different container frequencies ( $f_d$ ) and accelerations. The amplitude of a mode can be further excited by either frequency modulation of  $f_d$  or reduction of friction between the grains and the plate. When the mode amplitude becomes large, the lattice melts (disorders), in accord with the Lindemann criterion for melting in 2D.

Systems driven away from thermodynamic equilibrium often form patterns when forced beyond a critical threshold. Close to this bifurcation, the dynamics of large length scale perturbations to the wavelength of the patterns are well described by partial differential equations called amplitude equations, whose form is universal [1]. However, these equations lose predictive power for larger forcing. As an alternative description of patterns, Umbanhowar *et al.* [2] postulated that certain patterns could be described as a collection of localized interacting elements, the “atoms” of the patterns. This approach would replace the description of patterns by partial differential equations with a possibly simpler description based on a finite set of coupled ordinary differential equations. In this paper we show that the dynamics of square patterns formed in a thin layer of oscillated granular material can be described using concepts from lattice dynamics. This description provides a prediction of pattern behavior away from the bifurcation: the loss of long range order.

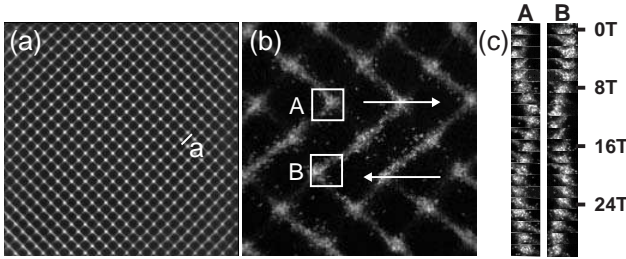


FIG. 1: (a) A lattice pattern strobed at  $f_d/2$  and averaged over 10 pattern oscillations ( $\Gamma = 2.90$  and  $f_d = 25$  Hz, parameters for which the lattice is almost motionless). The image shows the entire container,  $18 \times 18 \text{ cm}^2$ . (b) Close up snapshot image at  $\Gamma = 2.90$  and  $f_d = 30$  Hz, for which the lattice oscillates vigorously. (c) The time evolution of the peaks in boxes A and B in (b); these peaks oscillate out of phase with a frequency about 10 times smaller than the pattern oscillation frequency.

**Experiment.** A layer of 0.165 mm diameter bronze spheres [3] was oscillated at drive frequency  $f_d$  with non-dimensional peak plate acceleration  $\Gamma = A(2\pi f_d)^2/g$ , where  $A$  is the amplitude of the plate oscillation and  $g$  is the gravitational acceleration. For the layer depth studied (4 particle diameters), square patterns formed for

$2.5 < \Gamma < 4.0$  and  $f_d < 36$  Hz. The granular surface was imaged using low angle illumination that created bright regions at the peaks [4]. The scattered light was collected by a 256x256 CCD camera. To test for boundary effects, the experiments were conducted in two different containers, a circular cell with diameter 7 cm and a square cell 18 cm on a side. The results were the same in both containers, except that the circular container allowed the pattern to form with any orientation, while in the square container the patterns formed preferentially at  $\pi/4$  to the sidewalls.

**Lattice pattern.** The square patterns, illustrated in Fig. 1, oscillate subharmonically at  $f_d/2$ ; after each plate oscillation, a peak becomes a crater. At the phase in the plate oscillation cycle where the pattern amplitude is maximum, the pattern is composed of an array of peaks arranged in a square lattice connected by a network of thin lines of particles (Fig. 1(a)). At maximum height each peak typically contains several hundred particles. Images are collected at this phase in the cycle. In the dark regions between the peaks, there are almost no grains. Thus, when strobed at  $f_d/2$ , the pattern resembles a two-dimensional square crystal lattice made of discrete elements separated by lattice constant  $a$ . In this paper, we only consider the strobed motion of the lattice pattern.

**Lattice oscillation.** Even in the strobed frame, the lattice may not be stationary — the center of mass of each peak can oscillate around its lattice site, defined as the position of the peak, time-averaged over several hundred oscillations. The motion of a peak about its lattice site is periodic for a wide range of parameters, but for other parameter ranges the motion appears to be random, like that of a lattice in contact with a thermal bath. An example of periodic motion of the peaks is shown in Fig. 1(b) and (c), where rows oscillate exactly out of phase with each other. All of the peaks within a row at an angle  $\pi/4$  to the natural lattice direction maintain a constant separation of  $\sqrt{2}a$  during the oscillation; this is an example of a transverse mode in the (1, 1) lattice direction.

**Dispersion relation.** In general the lattice dynamics is more complicated than in Fig. 1. The dynamical behavior is determined from three-dimensional discrete Fourier transforms of a time series of images, giving  $\tilde{I}(k_x, k_y, f_L)$ ,

as shown in Fig. 2(b) and (c) for two lattice oscillation frequencies  $f_L$ ). The lowest order phase modulations of the square lattice are observed only in a direction  $\pi/4$  (or the degenerate  $3\pi/4$ ) relative to the lattice basis.

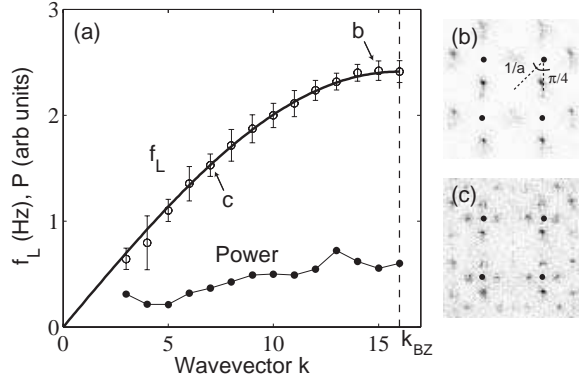


FIG. 2: (a) Comparison of the measured dispersion relation (o) at  $f_d = 25$  Hz and  $\Gamma = 2.75$  for the  $(1, 1)_T$  normal modes of the lattice with a one-dimensional lattice model (solid line) with transverse harmonic coupling between  $(1, 1)$  rows. The wavevector  $k$  is in units of  $4\pi/(\sqrt{2}aN)$ , where  $a$  is the lattice constant and  $N = 34$  is the number of  $(1, 1)$  rows in our square container. The dashed line denotes the edge of the first Brillouin zone for the  $(1, 1)$  direction of the positive values of  $k$ . (b) and (c) show the modulus of the spatial Fourier transforms,  $|\tilde{I}(k_x, k_y, f_L)|$ , at two lattice oscillation frequencies,  $f_L = 2.3$  Hz and  $f_L = 1.2$  Hz respectively; the former is close to the edge of the Brillouin zone. The sidebands represent the spatial modulation of the lattice  $\pi/4$  from the basic square lattice direction—the  $(1, 1)$  modes. The four peaks (•) that form the basic square lattice (found at  $f_L = 0$  Hz) have a power about 50 times larger than the background. The modes near the corners of the image in (c) are harmonics of the basic modulation.

In the language of lattice dynamics, the  $\pi/4$  and  $3\pi/4$  sidebands are the  $(1, 1)$  and  $(1, -1)$  modes of the lattice, respectively. We find that only the transverse modes,  $(1, 1)_T$  and  $(1, -1)_T$ , are excited (*e.g.* see Fig 1(b)). Their dispersion relation, determined by finding the modulation wavevector with maximum power for each  $f_L$ , is shown in Fig. 2(a). Since we do not know the form of the coupling between the lattice elements, we compare the data to a simple one-dimensional lattice model in which we assume that each  $(1, 1)$  row is harmonically coupled to its nearest  $(1, 1)$  neighbors [5]. The data are well fit by the dispersion relation for  $N$  harmonically coupled  $(1, 1)$  rows of peaks with boundary conditions such that a row next to the wall is connected to the wall by a spring. This yields  $f_L = f_{BZ}|\sin(ka/(2\sqrt{2}))|$ , where  $f_{BZ}$  is the frequency at the edge of the Brillouin zone,  $a$  the lattice spacing, and  $k = \frac{n\pi\sqrt{2}}{aN}$  is a wavevector in the  $(1, 1)$  direction [6]. Here  $N$  represents the number of  $(1, 1)$  rows of peaks in the lattice with  $1 \leq n \leq N$ , where  $N = 34$  (in Fig. 1,  $N = 32$ ); only  $N/2$  positive  $k$  modes are shown in Fig. 2(a) since the modes are decomposed into pe-

riodic Fourier components. We cannot resolve the low frequency modes ( $n = 1, 2$ ) because of variation in illumination over large length scales.

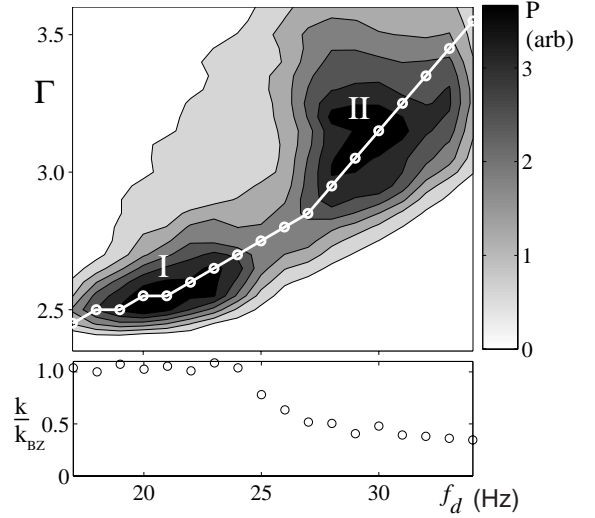


FIG. 3: Normal modes of the lattice exhibit two resonance peaks, I and II. Top panel: the grayscale indicates the power in the most intense mode. Bottom panel: The dominant excited wavevector normalized by the wavevector of the first Brillouin zone. The points are taken along the path in the top panel.

*Resonant modes.* For the value of  $\Gamma$  and  $f_d$  in Fig 2, the power is roughly independent of the mode number, indicating that the system is in contact with the equivalent of a thermal bath. However, in two ranges of  $\Gamma$  and  $f_d$ , certain modes become very intense, as Fig. 3 illustrates. The strength of the resonance regions labelled I and II in Fig. 3 was obtained by integrating the spectral power above the background that arises from motion of defects in the pattern on a time scale longer than the measurement time. Far from the two resonances, the lattice is nearly stationary, with small amplitude incoherent oscillations of the lattice elements around the mean sites.

The bottom panel of Fig. 3 shows the dependence of the wavevector of the dominant mode as a function of  $f_d$ . In resonance I, the power is dominant in the mode at the edge of the  $(1, 1)$  Brillouin zone,  $k = k_{BZ} = 2\pi/\sqrt{2}a$ , while in resonance II, the power is dominant in a mode near the middle of the Brillouin zone. Between the resonance peaks, around  $f_d \approx 26$  Hz, the total power is small and is distributed fairly uniformly among the modes, as Fig 2 illustrates. The measured dispersion relations are well-fit by the harmonically coupled lattice model for almost all  $(\Gamma, f_d)$ . We find that  $f_{BZ}$  (proportional to the square root of the ratio of effective spring constant to the effective mass of a  $(1, 1)$  row) varies between 1.5 and 2.5 as  $\Gamma$  and  $f_d$  are changed. We note that near the peaks of the resonances, the power is input dominantly in one mode; thus the signal-to-noise is not large enough to re-

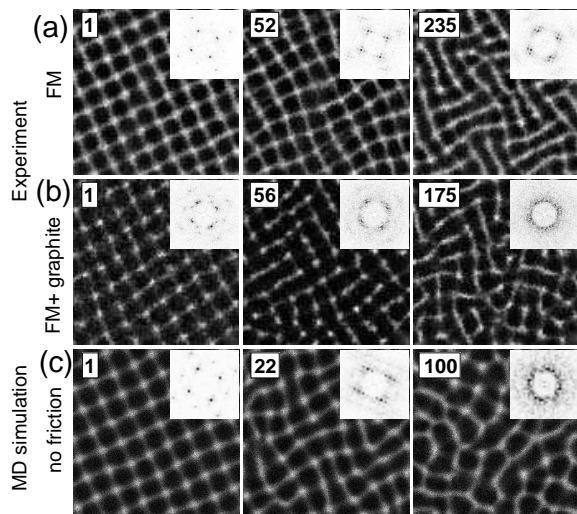


FIG. 4: Defect creation and melting for three cases after a sudden change in the system parameters. The numbers are the number of oscillations after the change in conditions, and the insets show the structure factor corresponding to the pattern. (a) At  $t = 0$ , frequency modulation with  $f_{mr} = 2$  Hz and  $f_{ms} = 5$  Hz was applied ( $\Gamma = 2.90$ ,  $f_d = 32$  Hz, which is in the weakly oscillating regime). (b) At  $t = 0$ , the same frequency modulation as in (a) was applied for particles which had been cleaned and graphite had been added. (c) Molecular dynamics simulation: at  $t = 0$ , the friction coefficient  $\mu$  between the grains and the plate was set to 0 ( $\Gamma = 3.0$  and  $f_d = 32$  Hz, which is in the weakly oscillating regime when  $\mu = 0.5$ ).

solve the dispersion relation for the other modes.

*Disorder and Frequency Modulation.* Near the maximum of resonance II, the amplitude of the mode that is resonantly excited is large enough to locally break the lattice and form defects. The defects either remain in the lattice or travel through the crystal and annihilate at the boundary. The defect creation rate (thus the disorder in the lattice) can be enhanced by resonantly exciting modes further using frequency modulation of  $f_d$  with modulation rate  $f_{mr}$  and modulation span  $f_{ms}$ . The signal applied to the shaker has the form,  $y = A \sin(2\pi f_d t + \frac{f_{ms}}{f_{mr}} \sin 2\pi f_{mr} t)$ . The lattice responds to the frequency modulation at exactly  $f_{mr}/2$ , and the strength of the response increases as  $f_{ms}$  increases.

The effect of frequency modulation is shown in Fig. 4(a), where  $f_{mr}$  is set to be twice the frequency of the mode at resonance II,  $f_L \approx 1.5$  Hz. Several hundred oscillations after the modulation is turned on, the amplitude of the excited mode becomes quite large, and a few defects are created. We have found that the disordering process is enhanced by washing the bronze particles with acetone and methanol in an ultrasonic cleaner and adding a small amount of fine graphite powder to the particles [7]. Before applying the frequency modulation, the grains are shaken for  $10^5$  oscillations to en-

sure uniform coating of the particles. After the frequency modulation is applied, the amplitude of the mode grows large enough to completely disorder the lattice, creating a melted liquid-like time-dependent pattern, as shown in Fig. 4(b).

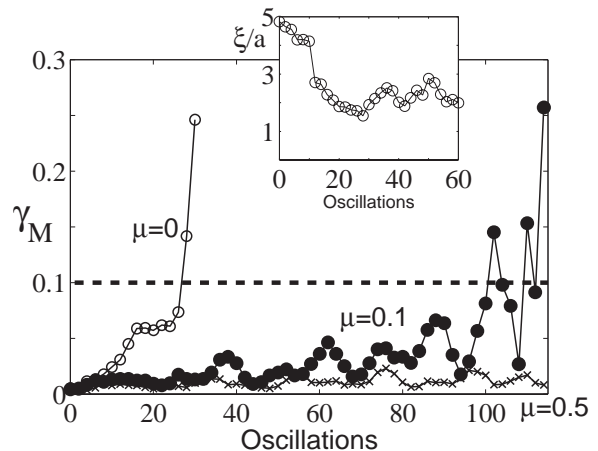


FIG. 5: Melting occurs when the Lindemann ratio  $\gamma_M$  (see text) reaches approximately 0.1. Main figure:  $\gamma_M$  versus time for different values of the friction coefficient  $\mu$  in simulations with  $\Gamma = 3.0$  and  $f_d = 32$  Hz. The inset shows that the correlation length of the pattern  $\xi$  ( $\circ$ ) for  $\mu = 0$  reaches the minimum value when  $\gamma_M \approx 0.1$ .

*Friction and Melting Criterion.* The addition of graphite presumably changed the friction in particle-particle and particle-boundary collisions; hence we have examined the role of friction on the behavior near the resonance peaks [8]. This was accomplished using an inelastic hard sphere molecular dynamics (MD) code since we could not change friction in a controlled way in the experiments. Previous work has demonstrated that the MD code generates patterns that match those observed for a wide range of  $\Gamma$  and  $f_d$  [9]. After the frictional coefficient [10] was reduced from  $\mu = 0.5$  to zero (cf. Fig. 4(c)), the amplitude of a mode began to grow. After about 30 plate oscillations, the amplitude became so large that the lattice disrupted and defects formed, leading to a liquid-like state. In this state, individual lattice elements underwent large nonperiodic displacements and were no longer confined to their respective equilibrium sites. Sometimes lattice elements annihilated or spontaneously created new peaks upon collision. In this melting process the correlation length  $\xi$  decreased from about  $5a$  to  $2a$  (see inset of Fig. 5).  $\xi$  was obtained by fitting an exponential to the envelope of the azimuthal average of the two-dimensional autocorrelation function. After reaching a minimum in about 30 plate oscillations,  $\xi$  oscillated about  $2a$  as the lattice continued to disrupt locally and heal.

Melting is observed in molecular dynamics simulations of two-dimensional solids when the Lindemann ratio,

$\gamma_M = \langle |u_m - u_n|^2 \rangle / a^2$ , exceeds 0.1 [11, 12]. Here  $u$  denotes displacements of atoms from lattice sites and the average is taken over all nearest neighbors  $m$  and  $n$ . We have computed the Lindemann ratio for the granular lattice from measurements of the motion of the peaks, and we have found that the lattice melts when  $\gamma_M > 0.1$ , just as in two-dimensional solids.

The melting that occurs when friction is switched off in the MD simulation occurs when  $\gamma_M$  increases through the value 0.1, as Fig. 5 illustrates. Thus, the melting indicated by the Lindemann criterion is in good accord with our observation of the decay of spatial correlations. For  $\mu = 0.5$ , the lattice never melts, while for  $\mu = 0.1$ , the pattern oscillates with increasing amplitude until local melting events disrupt the long-range order (Fig. 5). However, the value  $\mu = 0.1$  does not yield fully melted patterns, as the re-crossing of the  $\gamma_M \approx 0.1$  line indicates. After a defect is created, the mode amplitude becomes small at that position and the lattice can locally re-crystallize, preventing a transition to a fully liquid state. Note that our melting is driven by a resonantly excited mode of the lattice rather than thermal excitation, so our observations cannot be compared with the well-known two-dimensional melting theory of Halperin and Nelson [13], which requires thermal heating such that the power is distributed uniformly among all modes.

*Conclusions.* We have demonstrated that the square patterns in a vibrated granular layer behave like a two-dimensional lattice. The lattice approach can address questions such as melting, which cannot be addressed in an amplitude equation formalism. We conjecture that the stability exhibited by the nonequilibrium granular lattice pattern is an analog of “generalized rigidity” found in equilibrium lattice systems and discussed by Anderson [14]. Whether such concepts and predictive criteria can be applied to other nonequilibrium systems is an interesting open question. Finally, our observations of the effect of friction on melting of a granular lattice could be useful in guiding the development of kinetic and hydrodynamic theory of granular media, where the role of fric-

tion is not well understood [15].

We thank Paul Umbanhowar for helpful suggestions. This work was supported by the Engineering Research Program of the Office of Basic Energy Sciences of the U.S. Department of Energy.

---

\* goldman@chaos.ph.utexas.edu; URL: <http://chaos.ph.utexas.edu/~goldman>

- [1] M. C. Cross and P. C. Hohenberg, *Rev. Mod. Phys.* **65**, 851 (1993).
- [2] P. B. Umbanhowar, F. Melo, and H. L. Swinney, *Nature* **382**, 793 (1996).
- [3] The phenomenon was also observed in 0.165 mm diameter lead particles.
- [4] F. Melo, P. B. Umbanhowar, and H. L. Swinney, *Phys. Rev. Lett.* **75**, 3838 (1995).
- [5] C. Kittel, *Introduction to Solid State Physics* (Freeman, 1986), p. 82, 6th ed.
- [6] J. D. Louck, *Am. J. Phys.* **30**, 585 (1962).
- [7] Extra Fine Graphite powder manufactured by AGS Co, Muskegon, MI.
- [8] The addition of graphite increases the amplitude of the modes at the resonance peaks. In contrast, roughing the bottom plate (sandpaper grit 400 epoxied to the container bottom) decreases the amplitude of the resonances, allowing the formation of defect free patterns.
- [9] C. Bizon, M. D. Shattuck, J. B. Swift, W. D. McCormick, and H. L. Swinney, *Phys. Rev. Lett.* **80**, 57 (1998).
- [10] The value  $\mu = 0.5$  was found previously to yield patterns that match observations [9]; it is not necessarily the physical value of the friction coefficient.
- [11] V. Bedanov, G. Gadiyak, and Y. E. Lozovik, *Phys. Lett. A* **109A**, 289 (1985).
- [12] X. H. Zheng and J. C. Earnshaw, *Europhys. Lett.* **41**, 635 (1998).
- [13] B. I. Halperin and D. R. Nelson, *Phys. Rev. Lett.* **41**, 121 (1978).
- [14] P. W. Anderson and D. L. Stein, in *Basic Notions of Condensed Matter Physics*, edited by D. Pines (Addison Wesley Longman, Inc., 1997), p. 263.
- [15] J. T. Jenkins and C. Zhang, *Phys. Fluids* **14**, 1228 (2002).